

**NrdH-REDOXIN MEDIATES HIGH ENZYME ACTIVITY IN MANGANESE-RECONSTITUTED RIBONUCLEOTIDE REDUCTASE FROM *Bacillus anthracis***

**Mikael Crona<sup>1</sup>, Eduard Torrents<sup>1,2§</sup>, Åsmund K Røhr<sup>3§</sup>, Anders Hofer<sup>4</sup>, Ernst Furrer<sup>1#</sup>, Ane B Tomter<sup>3</sup>, K Kristoffer Andersson<sup>3</sup>, Margareta Sahlin<sup>1</sup> and Britt-Marie Sjöberg<sup>1\*</sup>**

From <sup>1</sup>Department of Molecular Biology and Functional Genomics, Arrhenius Laboratories for Natural Sciences, Stockholm University, SE-10691 Stockholm, Sweden, <sup>2</sup>Cellular Biotechnology, Institute for Bioengineering of Catalonia, Baldiri Reixac 15-21, ES-08080 Barcelona, Spain, <sup>3</sup>Department of Molecular Biosciences, University of Oslo, NO-0316 Oslo, Norway, <sup>4</sup>Department of Medical Biochemistry & Biophysics, Umeå University, SE-90187 Umeå, Sweden.

**Table of contents:**

Figures S1-S9

**Figure S1. The *B. anthracis* *nrdIEF* operon.** IVS denotes intervening sequence, and HEG denotes homing endonuclease gene. Primers described in Material & Methods and used for construction of the NrdE expression plasmid pETS146 are shown.

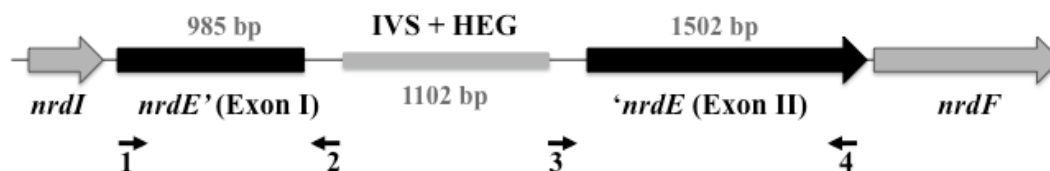


**Figure S2. SDS-PAGE of purified *B. anthracis* NrdE.** Lane 1, protein ladder (Fermentas); lane 2, crude extract (5  $\mu$ g) of *E. coli* culture overproducing *B. anthracis* NrdE; lane 3, purified *B. anthracis* NrdE (3  $\mu$ g).

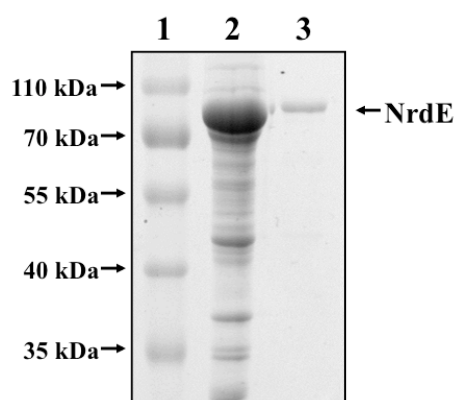


**Figure S3. Separation of *B. anthracis* NrdI from Mn-reconstituted NrdF using MonoQ anion exchange chromatography.** Separation of the NrdI protein and the NrdF protein with radical and lacking radical is indicated. The absorption is shown in mAU and the gradient from 0-60% 1 M KCl is shown.

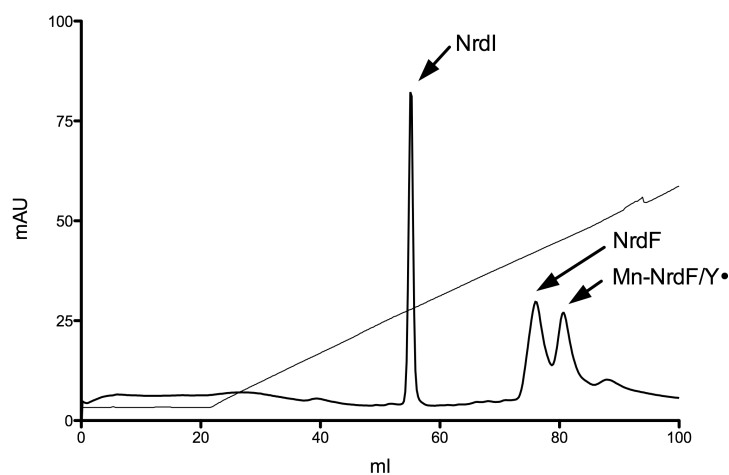


**Figure S4. Dithiothreitol and pH dependence of the *B. anthracis* RNR enzyme assay.** A) Dependence on dithiothreitol, B) dependence on pH. All incubations were done under standard conditions described in the material and methods using 7.4  $\mu\text{M}$  of NrdE and 16.2  $\mu\text{M}$  of Fe-NrdF.

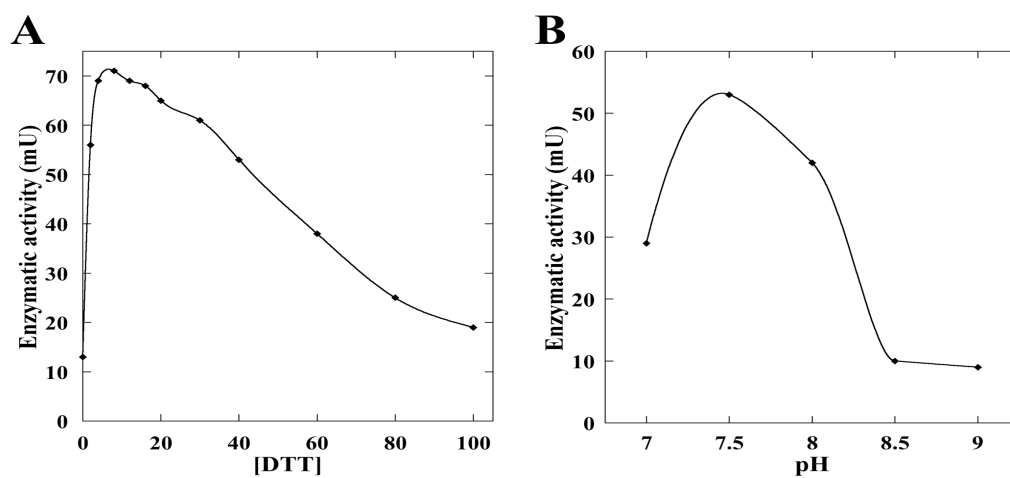


**Figure S5. *B. anthracis* NrdI/NrdF interaction SPR sensorgrams and steady state plots. 2.5  $\mu$ M-60  $\mu$ M of NrdI was injected over immobilized biotinylated NrdF proteins.**

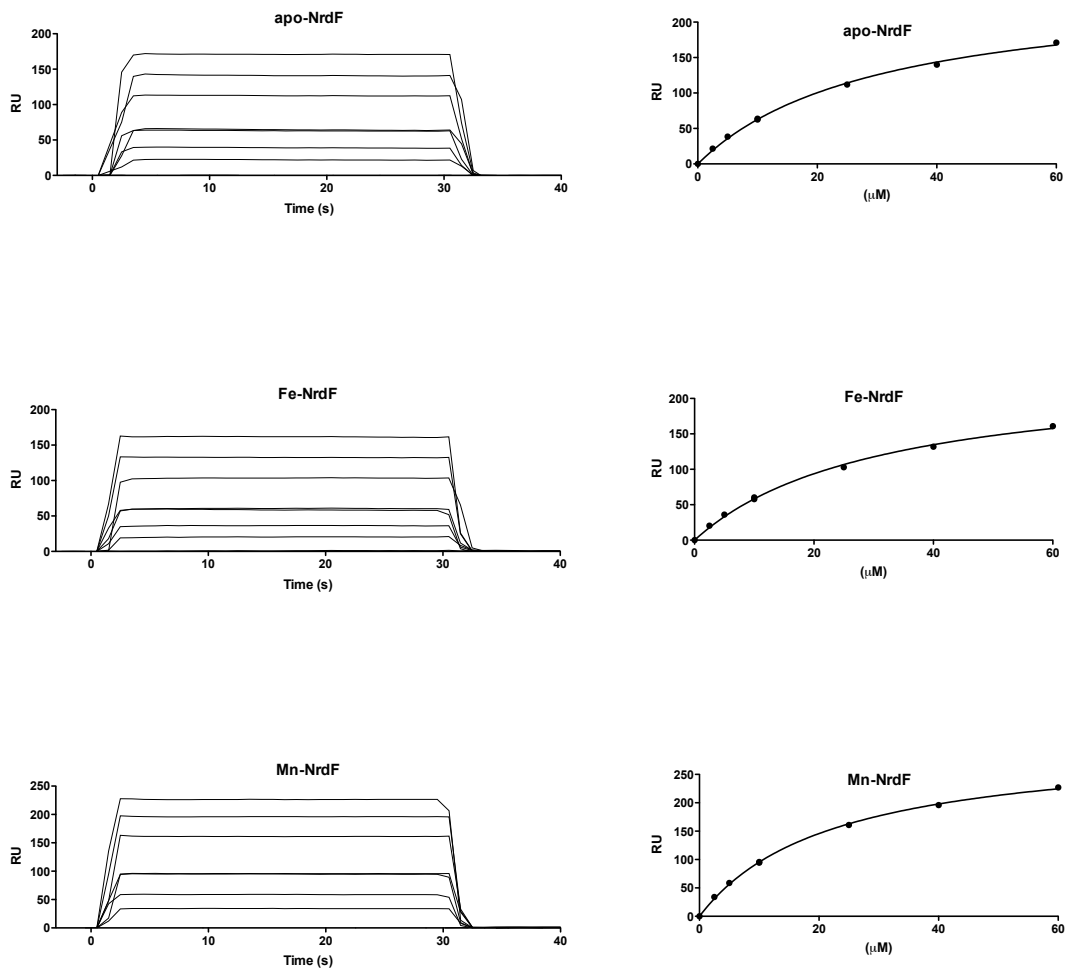


**Figure S6. *B. anthracis* NrdE/NrdF interaction SPR sensorgrams and steady state plots.** 0.025  $\mu$ M-2  $\mu$ M of NrdE was injected over immobilized biotinylated NrdF proteins.

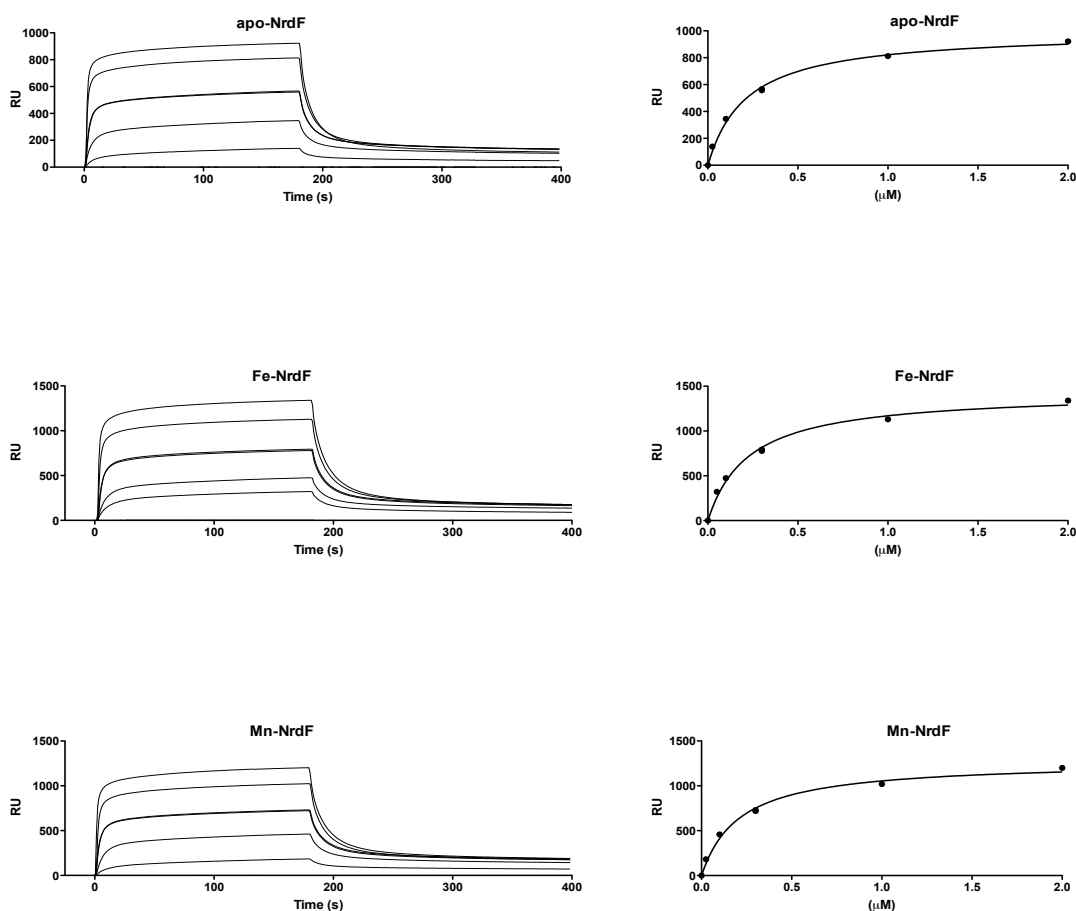


**Figure S7. Dimerization of *B. anthracis* NrdE is promoted by effectors but not by substrate.** GEMMA analyses of 0.02 mg/ml NrdE alone and in the presence 25  $\mu$ M dGTP, 50  $\mu$ M dTTP, or 50  $\mu$ M CDP. The composition and predicted sizes of the species (in kDa) are indicated.

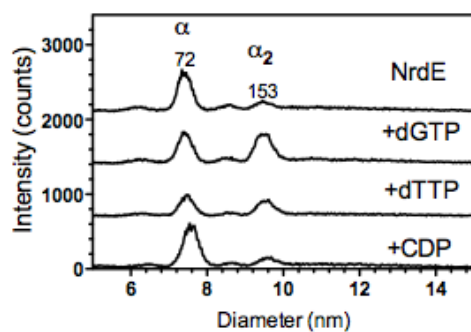


**Figure S8. Titration of *B. anthracis* NrdE+dTTP with increasing concentrations of Mn-NrdF.** GEMMA analyses of 0.02 mg/ml NrdE, 50  $\mu$ M dTTP, in the presence of varying concentrations of Mn-NrdF (0.0053 and 0.017 mg/ml). The composition and predicted sizes of the species (in kDa) are indicated.

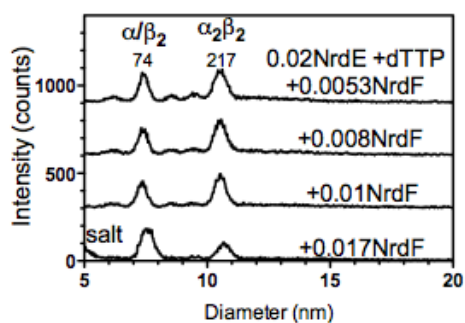


**Figure S9. Activity of *B. anthracis* NrdF in presence of increasing NrdI concentrations.** The activity of Fe and Mn reconstituted *B. anthracis* NrdF proteins were only marginally effected by an NrdI excess of up to 8 times. Specific activity in absence of NrdI: Mn-NrdF 67.83 U/mg and Fe-NrdF 10.67 U/mg.

